

Stagnation Temperature Effect on the Flow in the Supersonic Axisymmetric Minimum Length Nozzle with Application for Air

Mohamed Roudane*, Toufik Zebbiche**, Mohamed Boun-jad***

Keywords : Axisymmetric Minimum Length Nozzle, High temperature, Cubic spline interpolation method, Predictor corrector algorithm, Method of Characteristics, Flow parameters.

ABSTRACT

The work is to develop a new numerical calculation program to do the correction of the flow parameters in a supersonic axisymmetric minimum length nozzle, dimensioned on the basis of use of ideal gas assumptions at constant C_p , giving a uniform and parallel flow at the exit section, by using the model at high temperature of C_p variable with the temperature, lower than the threshold of dissociation of the molecules. The shape of the nozzle does not change. It is determined by using the method of characteristics. Only the behavior of the gas exchange and regards itself as a high-temperature gas. It shows that the flow at the exit section of the nozzle is no more uniform and parallel and one will find a degradation of this parameter. Also the flow through the nozzle will be completely changed in comparison with that given by the PG model and in particular the coefficient of the pressure force will be fixed. All flow parameters depend on the stagnation temperature and the exit Mach number. Error caused by the perfect gas model over to high temperature model is calculated. The application is for air.

INTRODUCTION

The supersonic nozzles are used to accelerate the gas from the combustion end to supersonic speed to generate some thrust force as a result of this
Paper Received June, 2016. Revised September, 2016, Accepted October, 2016, Author for Correspondence: Toufik Zebbiche.

* Doctor, Department of Mechanical Engineering, Faculty of Technology, University of Blida 1, BP 270 Blida 09000, Algeria.

**Professor, Institute of Aeronautics and Space Studies, University of Blida 1, BP 270 Blida 09000, Algeria.

*** Doctor, Department of Mechanical Engineering, Faculty of Technology, University of Blida 1, BP 270 Blida 09000, Algeria.

acceleration. From Anderson (1982), Peterson and Hill (1965) and Zuker (2002), several types of nozzles are in the literature. Usually we are interested in nozzles giving a uniform and parallel flow at the exit section Argrow (1988) and Anderson (1988). Several models are used for the design of supersonic nozzles. Noting the model of an ideal gas as presented in Peterson and Hill (1965), Argrow et al. (1988), Dumitrescu (1975) and Emanuel (1975) and for the HT models presented in Zebbiche (2007a, 2011, 2007b, 2007c, 2006). The authors are interested in the MLN nozzle type, see figure 1. Such nozzle gives a minimum length comparing with the standard nozzle expansion area Peterson and Hill (1965).

For aeronautical applications, whether missiles and supersonic aircraft engines use the model of an ideal gas to the used nozzle design Peterson and Hill (1965) and Emanuel (1986). This model is used by several manufacturers, since there is no other specific model before the development of HT model Zebbiche (2011), Zebbiche and Youbi (2007c) and Zebbiche and Boun-jad (2012) close to the real case. Among the conclusions drawn from Zebbiche (2011) is that the PG model gives good results when $T_0 < 1000$ K, whatever $M_E < 2.00$ regardless of T_0 . This limit is insufficient to meet the needs when $T_0 > 1000$ K.

When $T_0 > 1000$ K, the gas physically behaves like a gas at HT . The assessment of the conservation of energy exchange. But the assumptions made by manufacturers when they made the design on the bottom of the ideal gas model give significant errors in the design parameters.

Zebbiche (2011) and Zebbiche and Youbi (2007c), developed a model based on the method of characteristics to find a form of the nozzle as a correction to the forms of PG model.

Noting that the PG model gives no information on the effect of T_0 on the nozzle design. The problem is that if we keep the same shape of the MLN nozzle sized on the basis of PG model, giving a uniform and parallel Mach number at the exit section, this is what really delivers the same exit Mach number, plus it is still uniform and parallel to the exit section if one takes into account T_0 . Especially if the temperature is high.

Most of the software found in the literature that are based on solving the Euler equations are developed

on the basis of the use of perfect ideal gas. We speak mainly on the equation of conservation of energy which must be modified to take into account the variation of C_p which in this case will vary with the temperature for the HT model. So our goal is to use the HT model to calculate the correction to the flow parameter through the axisymmetric MLN nozzle, sized on the basis of the PG model presented in Peterson and Hill (1965), Argrow and Emanuel (1988) and Dumitrescu (1975) by the MOC method and determine the error made by the PG model compared to the HT model. The application is for air.

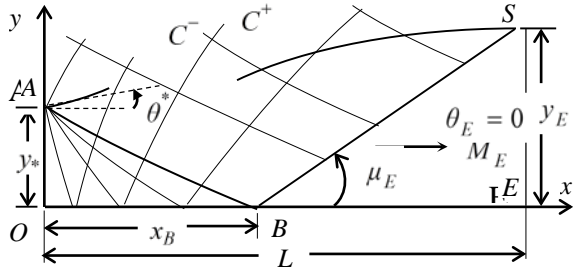


Fig. 1 Flow field inside the axisymmetric PG MLN.

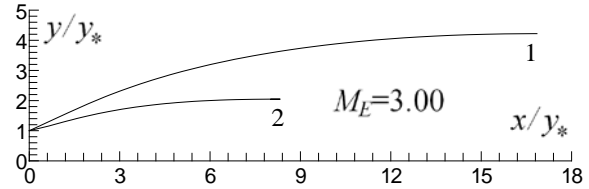
From figure 1, it is noted that the flow field in the nozzle is divided into three zones. We find the region OAB, appointed by Kernel region of non simple type. The region ABS, appointed by transition region is of not simple. The last region BES triangular shape is made uniform. So our contribution will demonstrate that this indicated subdivision will disappear, and we will find only one single flow area of not simple type, fully into the nozzle. Then we will see a change so the C_f . Zebbiche (2011) and Zebbiche and Youbi (2007c), to keep the same C_f and M_E , they determine another form of the nozzle larger than the nozzle of an ideal gas. In other words, the exit section will be high. This is logical. If we keep the same shape of the nozzle of the PG model, there will be a change in performance. A study will be made in this case to visualize the difference.

If we want to make experience on a supersonic flow over aircraft in a supersonic wind tunnel formed by the nozzle of figure 1, the aircraft will not be placed in terms of the uniform and parallel upstream Mach number. In this case the actual flow which is uniform and parallel will not be modeled, especially if $T_0 > 1000K$.

MATHEMATICAL FORMULATION

The figure 2 shows the shape of the nozzle obtained by using for the PG model, and giving a uniform and parallel flow at the exit section. The example chosen is $M_E = 3.00$ for air and $\gamma = 1.402$. So in this case, the length and exit radius of the nozzle are equal to $L/y_* = 8.355$, $y_E/y_* = 2.054$ as presented in Peterson and Hill (1965), Argrow and Emanuel (1988), Dumitrescu (1975) and Zebbiche (2007a).

The used Compatibility equations by the MOC are presented in Argrow and Emanuel (1988), Zebbiche and Youbi (2007b), Zucro and Hoffman (1976) and Oosthuisen and Carscallen (1997). The shape of the nozzle is obtained point by point, in the form of tabulated values. Then to obtain an analytical equation $f(x)$ to the nozzle shape must be used to interpolate the points. In our work we chose to cubic spline interpolation.



Curve 1 : 2D Nozzle. Curve 2 : Axisymmetric Nozzle

Fig. 2 Contour of the PG MLN.

The calculation of the flow in the nozzle is effected by the use of compatibility and characteristics equations at HT, shown in Zebbiche (2011), summarized by:

$$\begin{cases} \frac{C_p(T)}{2H(T)} \sqrt{M^2(T)-1} dT + d\theta = \frac{\sin\theta \sin\mu}{y \cos(\theta-\mu)} dx \\ \frac{dy}{dx} = \tan(\theta-\mu) \end{cases} \quad (1)$$

$$\begin{cases} \frac{C_p(T)}{2H(T)} \sqrt{M^2(T)-1} dT - d\theta = \frac{\sin\theta \sin\mu}{y \sin(\theta+\mu)} dx \\ \frac{dy}{dx} = \tan(\theta+\mu) \end{cases} \quad (2)$$

Where

$$H(T) = \int_T^{T_0} C_p(T) dT \quad (3)$$

$$\mu = \arcsin\left(\frac{1}{M}\right) \quad (4)$$

Expressions of $C_p(T)$ and R are presented in Zebbiche (2011), Zebbiche and Youbi (2007a, 2007b, 2007c).

Equations (1) are valid on the Mach line ζ , and equations (2) are valid on the Mach line η as present in figure 3.

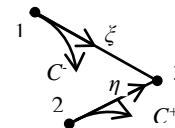


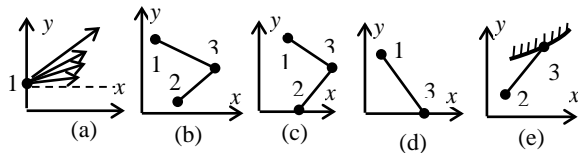
Fig. 3 Downward and upward Mach lines.

While four equations with four unknowns are obtained (x, y, θ and T) at each point 3 of the flow fields. Solving the system of equations (1) and (2) is made by the finite difference method with predictor corrector algorithm Argrow and Emanuel (1988), Emanuel

(1986), Zebbiche (2011) and Zebbiche and Youbi (2007c). This algorithm makes successive iterations of a proposed initial solution. This solution is taken to be the average of the results for nodes 1 and 2 which are related to the node 3. The number of iterations performed is of the order of 8 to 14 iterations. It depends grid generated in the nozzle and the accuracy of results evolves. While the stability of digital process is guaranteed and no divergence of results is observed.

We can have five types of flow points as the following figure 4. The flow parameters in the points 1 and 2 are known. The problem is to determine the parameter at point 3.

The wall has an inclination at initial point, designated by θ^* , as present in figure 1. At the throat OA we have $M=1.00$. The calculation process from the expansion center is shown in figure 5. Endless Mach wave are derived from the point A . Point A is therefore a point of discontinuity in parameter, such as the Mach number. It requires following the calculation of flow parameters at point 3 of figure 4.



- (a) : Expansion center point (Point A in figure 1).
- (b) : Regular internal point.
- (c) : Particular Internal point.
- (d) : Point on the axis of symmetry.
- (e) : Point on the wall of the nozzle.

Fig. 4 Different points of the flow field.

If N points are on a downward characteristic of the wall, then the first point will be processed using the procedure of a point on a rigid wall, see figure 4e. The last point will be treated as a point on the axis of symmetry, see figure 4d. The penultimate point will be treated as a particular internal point, see figure 4c. Here $\sin(\theta)/y$ in equations (2) becomes indeterminate (0/0). We must to resolve this problem Zebbiche (2011). The remaining points will be treated using the process of a regular internal point, see figure 4b. The accuracy of calculation descending depends on the number of characteristics descending from the center A . For supersonic flows, the flow parameters at a point depends only on the upstream conditions irrespective of the downstream conditions.

Figure 5 shows the process of calculating the flow parameters from the expansion center A of figure 1. Point A is then a flow discontinuity point since it belongs to all the downstream characteristic. Incrementing the deflection of the flow is made to point A formed each time in a following downstream C .

Once the calculation is complete from expansion center A , which represents the downstream characteristic line shown in figure 6a, we calculate the flow properties of the points of intersection of descendants C from the wall of the nozzle as presented in figure 6. The process

of calculating the flow from the wall is shown in figure 6. The calculation in the area of the wall will stop when reaches the last point S of figure 1.

For the point on the wall of the nozzle (figure 4e) and point 3 in the figure 6a, equations (2) will only be used to determine the parameters in point 3. The values of y_3 and θ_3 will be determined by the following relations, which will be added to equations (2) to obtain 4 equations with 4 unknowns.

$$\theta_3 = \arctg(f'(x_3)) \quad (5)$$

$$y_3 = f(x_3) \quad (6)$$

For the point on the axis of symmetry (figure 4d) was $\theta_3=0.0$ and $y_3=0.0$. Only then equations (1) will be used to determine the parameters x_3 and T_3 . Then for each point in figure 4, the unknowns are x_3, y_3, θ_3 and T_3 . Other parameters such as $M_3, P_3/P_0$ and ρ_3/ρ_0 can be determined by the following relations Zebbiche (2011) and Zebbiche and Youbi (2007b, 2007c) when T_3 is determined:

$$M_3 = \frac{\sqrt{2 H(T_3)}}{a(T_3)} \quad (7)$$

$$a(T_3) = \sqrt{\gamma(T_3) R T_3} \quad (8)$$

$$\frac{\rho_3}{\rho_0} = \text{Exp}\left(-\int_{T_3}^{T_0} C_p(T)/a^2(T) dT\right) \quad (9)$$

$$\frac{P_3}{P_0} = \left(\frac{T_3}{T_0}\right) \left(\frac{\rho_3}{\rho_0}\right) \quad (10)$$

$$\gamma(T_3) = \frac{C_p(T_3)}{C_p(T_3) - R} \quad (11)$$

$$\left(\frac{y_E}{y_*}\right)^2 = \frac{1}{M_E} \left[\frac{2}{\gamma+1} \left(1 + \frac{\gamma-1}{2} M_E^2\right) \right]^{\frac{\gamma+1}{2(\gamma-1)}} \quad (12)$$

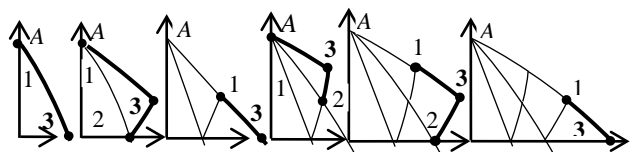


Fig. 5 Calculation process of characteristics from expansion center.

Equations (7), (8), (9) and (11) are those of HT model. The relationship between M_E and the radius of the exit section of figure 2 is given by equation (12), because the nozzle is sized on the basis of PG model Anderson (1982), Peterson and Hill (1965), Argrow and Emanuel (1988), Dumitrescu (1975), Emanuel (1986) and Oosthuisen and Carscallen (1997).

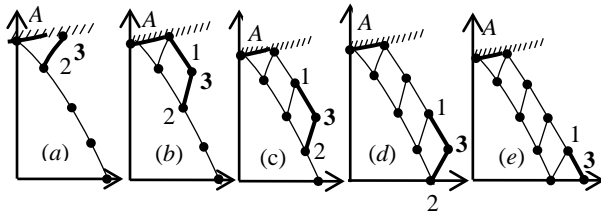


Fig. 6 Calculation process from the wall.

Once the parameters are calculated (M, T, P and ρ) at each point through the wall of the nozzle, we can be calculated by following relationship Berger (1978), Démidovitch and Maron (1987), Fletcher (1988), McLain (1975), Raltson and Rabinowitz (1985), the thrust coefficient C_F when the gas is used instead of air :

$$C_F = \sum_{j=1}^{j=N-1} \left(\frac{P_{(j)}}{P_0} \right) \left(\frac{S_{(j)}}{A_*} \right) \sin(\theta_{(j)}) \quad (13)$$

The terms in equation (15) are given by :

$$P_{(j)} = \frac{P_j + P_{j+1}}{2} \quad (14)$$

$$\frac{S_{(i)}}{A_*} = \left(\frac{y_i + y_{i+1}}{y_*} \right) \left[\left(\frac{x_{j+1} - x_j}{y_*} \right)^2 + \left(\frac{y_{j+1} - y_j}{y_*} \right)^2 \right] \quad (15)$$

$$\theta_{(j)} = \arctg \left(\frac{y_{j+1} - y_j}{x_{j+1} - x_j} \right) \quad (16)$$

PARAMETERS THROUGH THE EXIT SECTION

Selecting the parameters of the flow through the exit section of the nozzle of figure 2 are constant if the PG model calculation is used. But if the HT model is taken into account, which is actually the case if T_0 is high, determine the new parameter variation across the exit section, and look at the influence of T_0 on all parameters, including M and θ .

To get results, we must first identify all segment so mesh crossing the exit section. The various possible cases of segments are shown in figure 7.

The problem is to determine the parameter values ($y, M, \theta, T, \rho/\rho_0, P/P_0$) in this section points in the segments of the characteristics that intersect at the exit section, not to mention the point on the symmetry axis ($y=0, \theta=0$) and the point on the wall. It can have the following three options:

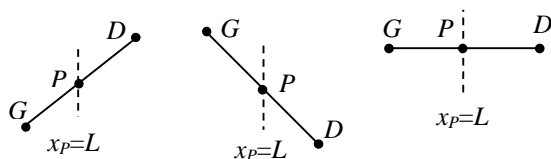


Fig. 7 Different segments of the search of points.

The problem is to determine the properties ($y, M, \theta, T, \rho/\rho_0, P/P_0$) at the point P , knowing $x_P=L$. The properties at the points G and D are already determined during the calculation of the internal flow by the use of MOC/HT model.

To know what is on the downward or upward characteristic or on the axis of symmetry, we made the following test:

$$\Delta y = y_D - y_G \quad (17)$$

If $\Delta y > 0$, one is on the upward characteristic C^+

If $\Delta y < 0$, one is on the downward characteristic C^-

If $\Delta y = 0$, one is on the symmetry axis.

To detect the segment containing the point P of the section $x_P=L$, it must satisfy the following condition:

$$(L - x_G) \cdot (L - x_D) \leq 0 \quad (18)$$

Note that the shape of the nozzle remains unchanged; only the behavior of the fluid changes with T_0 . First we must know the position of the point P , so we lack the ordinate this point. By writing equations between points G and P and the points G and D , we obtain:

$$y_P = \left[\frac{y_D - y_G}{x_D - x_G} \right] (x_P - x_G) + y_G \quad (19)$$

One can determine the parameters as at point P , if one interpolates two parameters from the set of parameters. We choose the angle θ and T . The other parameters will be deduced as a result. So, the point G is $S=0$ and the point D is at $S=S_{GD}$. The linear variation $\theta(S) = \alpha S + \beta$ and $T(S) = \alpha' S + \beta'$ between the point G ($S=0, \theta=\theta_G, T=T_G$) and point D ($S=S_{GD}, \theta=\theta_D, T=T_D$) gives the angle θ_P at point P by:

$$\theta_P = \frac{S_{GP}}{S_{GD}} (\theta_D - \theta_G) + \theta_G \quad (20)$$

$$T_P = \frac{S_{GP}}{S_{GD}} (T_D - T_G) + T_G \quad (21)$$

With S_{GP} and S_{GD} are given by equation (22) and (23).

$$S_{GP} = \sqrt{(x_G - x_P)^2 + (y_G - y_P)^2} \quad (22)$$

$$S_{GD} = \sqrt{(x_G - x_D)^2 + (y_G - y_D)^2} \quad (23)$$

The ratio of T/T_0 at point P can be obtained.

The calculation of $M, \rho/\rho_0$ and P/P_0 at the point P are obtained respectively by (7), (9) and (10) by replacing $T_3=T_P, M_3=M_P, P_3=P_P$ and $\rho_3=\rho_P$.

For tracing each parameter according to the ordered exit section must sort the points in order of increasing or decreasing the ordered y_P .

PARAMETERS THROUGH THE AXIS OF SYMMETRY

We are interested only in this case the grid points that lie on the axis of symmetry. Condition to detect

these points is $y_p=0.0$. No interpolation is done in this case. Then the flow parameters ($x_p, y_p=0.0, \theta_p=0.0, M_p, T_p/T_0, P_p/P_0, \rho_p/\rho_0$) at these points are known. For the nozzle of figure 1, these parameters are constant in the area *BES* triangular.

PARAMETERS THROUGH THE WALL OF THE NOZZLE

Once we calculate the flow parameters on the first point of each characteristic down from the wall, see figure 7, these parameters are stored in a separate file. That way, we can trace the flow parameters depending on the horizontal x-axis of the nozzle.

ERROR CAUSED BY THE PG MODEL

The flow in the nozzle sized by the *PG* model is calculated using the *HT* model. Then the *PG* model will cause an error compared to *HT* model. For all flow parameters, one can determine the relative error between the two models by :

$$\varepsilon_{Parameter} (\%) = \left| 1 - \frac{parameter_{PG}}{parameter_{HT}} \right| \times 100 \quad (24)$$

RESULTS AND COMMENTS

The figures with containing 4 curves representing the variation of the relevant parameter for 3 margins of T_0 , which is 1000 K (curve 2), 2000 K (curve 3), 3000 K (curve 4). Curve 1 represents the variation of the parameter for the case of ideal gas for $\gamma=1.402$ for air. The results of the ideal gas curve 1 can be found in Peterson and Hill (1965), Argrow and Emanuel (1988), Dumitrescu (1975) and Zebbiche (2011).

The figures with containing 3 curves are considered to present the variation of the relative error for Mach number. While curve 1 represents the error caused by the *PG* model over the *HT* model when $T_0=3000$ K. Curve 2 for $T_0=2000$ K and curve 3 for $T_0=1000$ K.

Mesh in characteristics

Figure 8 shows a type of mesh of characteristics in an *MLN* nozzle for *PG* Model. This nozzle supplies a uniform and parallel flow at the exit section, since the gas through the nozzle acts as an ideal gas according to the *PG* model. It is clearly seen that the region of the flow is divided into three zones as presented in figure 1.

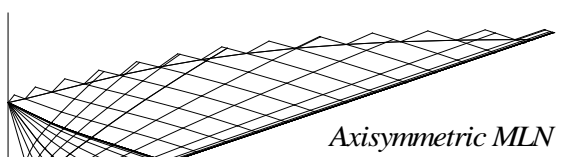
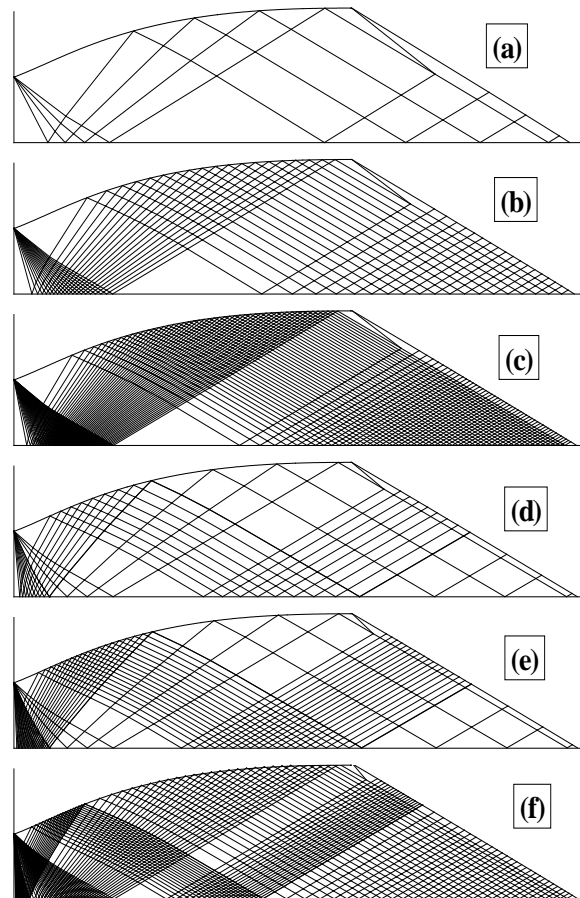


Fig. 8 Mesh for axisymmetric *PG MLN*.



- (a) : $NC=5, NJ=0$.
- (b) : $NC=20, NJ=0$.
- (c) : $NC=50, NJ=5$.
- (d) : $NC=5, NJ=10$.
- (e) : $NC=30, NJ=20$.
- (f) : $NC=50, NJ=20$.

Fig. 9 Mesh in characteristics of *HT* gas in *PG MLN*.

The mesh shown in figure 9 is presented to the *HT* model in a nozzle sized using the *PG* model. It represents the meshes in *MLN* axisymmetric nozzle when the gas behaves like as *HT* and that for different mesh parameters. In this case we note the disappearance of the three areas, and are replaced by only one single area not simple.

While figure 9a shows a large mesh with $NC=5$ *C*, and no *C* means is inserted ($NJ=0$) between the sonic line and the first regular *C*. In this case, the flow is poorly presented adjacent to the throat, and on the wall in the vicinity of the point A. In figure 9b we have $NC=20$. Same problem occurs in the vicinity of the wall and the throat of the nozzle, where the flow is miscalculated. We increased the *C* number in figure 9c until $NC=50$, and the same problem occurs on the wall at the throat, but with a least error with respect to figure 9b.

To solve this problem, it was inserted some *C* between the sonic line and the first regular *C* from the expansion center a respectively shown in figures 9d, 9e and 9f. If we look the shape of the mesh at the wall in the vicinity of throat, we note that the problem is solved

gradually especially if we increase the number NJ . It should be noted that for our applications, the meshes can go to $NC=4000$ and $NJ=350$.

Results for symmetry axis

Figure 10 shows the variation of the Mach number along the axis of symmetry of the nozzle. Consider the flow for HT model. Note that the Mach number increases from $M=1.00$ of the throat to M_E in case PG model and lower to M_E for the HT model.

More T_0 increases, the Mach number on the axis of symmetry at the exit section gradually decreases. We note that for curve 1, there is a horizontal line which is limited to $M_E=3.00$. This line represents the variation in the uniform area BES of figure 1. Since in this area, the flow is entirely uniform. But if the gas is regarded as HT , we note that in the BES area, the Mach number remains more constant. Adjacent to the throat, four curves are almost together, which shows the no influence of HT model on the Mach number, but closer to the end area of the Kernelregion, we can see the difference between the 4 curves, which shows the propagation of errors because the flow depends on the upstream conditions.

When $T_0=1000$ K, 2000 K and 3000 K, the Mach number at the exit section is respectively equal to 2.956, 2.872 and 2.845. So the PG model degrades the performance including M_E . The HT expansion becomes incomplete in the PG nozzle. There is a lack of space for complete expansion to $M_E=3.00$. To see a complete expansion, we must develop another form of the more spacious than the PG form to give the desired M_E .

Figure 11 shows the variation of the pressure ratio along the axis of the nozzle giving $M_E=3.00$ for the PG model. The same remarks concerning the variation of Mach number remain valid for the pressure ratio. At the exit section is equal to 0.0277, 0.030, 0.031 respectively for $T_0=1000K$, 2000K and 3000K and equal to 0.0272 for the PG model. We note that T_0 affects the increase in pressure ratio, which affects the increase of pressure force coefficient, see figures 27 and 29.

Figure 12 shows the variation of T/T_0 along the axis of the nozzle giving $M_E=3.00$ for the PG model. It is also on the axis of symmetry at the exit section have 0.380, 0.428, 0.450 respectively for $T_0=1000K$, 2000K and 3000K and equal to 0.355 for PG model. We note that T_0 affects the increase of T/T_0 .

Figure 13 shows the variation of the ratio ρ/ρ_0 along the axis of the nozzle giving $M_E=3.00$ for the PG model. We note that T_0 affects the increase in the ratio.

The error at each section through the axis of the nozzle is shown in figure 14. Note that the error can go to 10.31%, 8.78%, 3.71% for $T_0=3000K$, 2000K and 1000K which is about at the end of the Kernel region. The error at the exit section is equal 1.73%, 5% and 6.07% respectively for $T_0=1000K$, 2000K and 3000K. These values are found when $M_E=3.00$ of PG model. Then errors vary with the variation of M_E and T_0 .

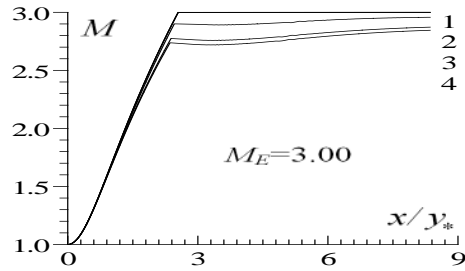


Fig. 10 Variation of the Mach number along the axial axis of the PG axisymmetric MLN .

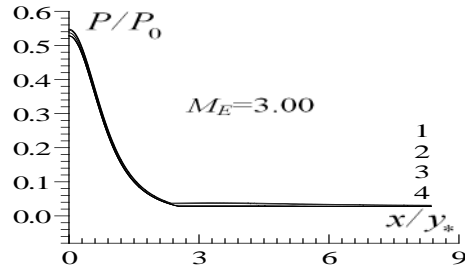


Fig. 11 Variation of the pressure ratio along the axial axis of the PG axisymmetric MLN .

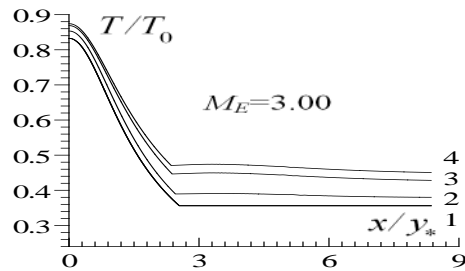


Fig. 12 Variation of the temperature ratio along the axial axis of the PG axisymmetric MLN .

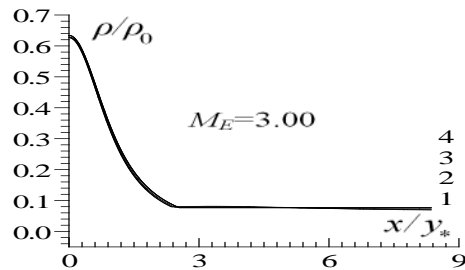


Fig. 13 Variation of the density ratio along the axial axis of the PG axisymmetric MLN .

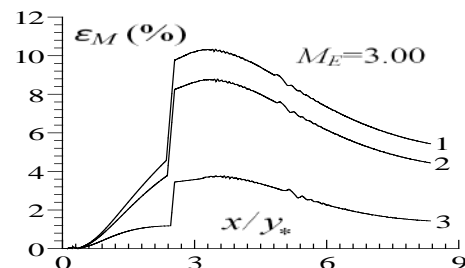


Fig. 14 Variation of the local relative error given by M on the axial axis of the PG axisymmetric MLN .

Variation on the wall of the nozzle

The figure 15 shows the variation of the Mach number along the wall of the nozzle. Soits shape does not change if the fluid behavior changes. Considering the flow HT , Was determined the change of Mach number witch increases from $M=1.00$ at the throat until exit Mach number equal to M_E for PG model and to Mach number lower than M_E for HT model. The Mach number at the center of expansion increases from $M=1.00$ until 1.477, 1.468 and 1.465 respectively for $T_0=1000K, 2000K$ and $3000K$ and equal to 1.493 for PG model.

More T_0 increases, theMach number on the wall of the nozzle at the exit section gradually decreases. As information, when $T_0=1000K, 2000K$ and $3000K$, the Mach number on the wall in the exit section is respectively equal to 2.918, 2.803 and 2.770. So the PG model degrades the performances including M_E . The HT expansion becomes incomplete in the PG nozzle. There is a lackof spaceforcomplete expansion to $M_E=3.00$. For curves 2, 3 and 4, in the vicinity of the exit section, we notice a degradation of Mach number, which justified by the birth of a weak oblique shock wave, as the Mach number immediately after the shock remains supersonic.The Mach number where there is a shock wave is equal to 2.925, 2.821, 2.789 respectively when $T_0=1000K, 2000K$ and $3000K$, and the Mach number immediately after the shock is estimated equal to 2.918, 2804, 2772. This degradation will further reduce other thermodynamic parameters. In some ways, we can say thatif the gas is considered as HT , the flow through the nozzle is not isentropic saw the birth of an oblique shock.

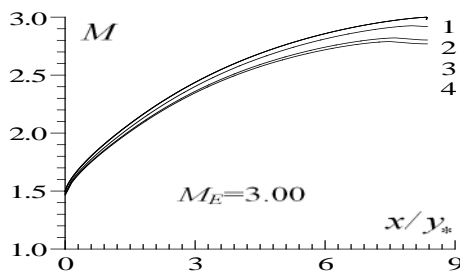


Fig. 15 Variation of the Mach number alongthe wall of the PG axisymmetric MLN .

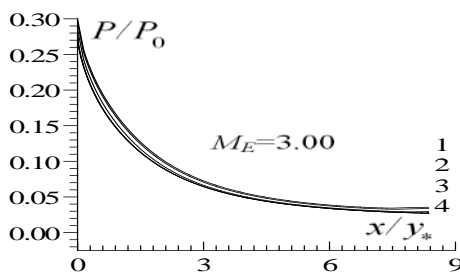


Fig. 16 Variation of the pressure ratio alongthe wall of the PG axisymmetric MLN .

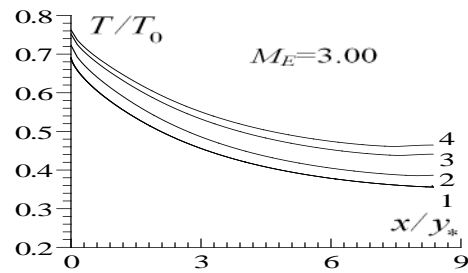


Fig. 17 Variation of the temperature ratio alongthe wall of the PG axisymmetric MLN .

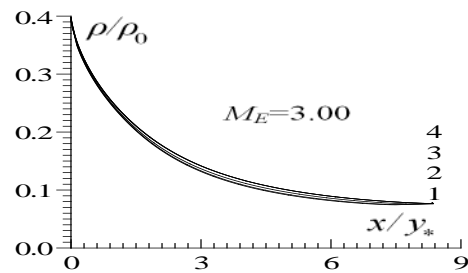


Fig. 18 Variation of the density alongthe wall of the PG axisymmetric MLN .

Note that the position of the shock is closer to the exit section, plus T_0 decreases, which means that the more we diminish T_0 , more shock will disappear and leaves the exit section. The flow in this case is purely isentropic. This is the case for the PG model. This is justified by the possibility of applying the PG model instead of HT model if $T_0 < 1000K$.

Sometimes it is use ful to truncate the nozzle at the position of oblique shock for not having a dissipation of the inner nozzle and the flow becomes purely isentropic. This cut will reduce somewhat the coefficient C_F but in parallelwe will win a percentage of the weight of the nozzle.

Figure 16 shows the variation of the pressure ratio along the wall of the nozzle giving $M_E=3.00$ for the PG model. The same remarks concerning the variation of Mach number remain valid for P/P_0 . It is equal on the wall at the exit section 0.029, 0.033, 0.035 respectively for $T_0=1000K, 2000K$ and $3000K$ and equal to 0.028 for the case of PG model. Note that the increase in T_0 has influenced the increase in P/P_0 ratio.

The figure 17 shows the variation of the ratio T/T_0 along the wall of the nozzle giving $M_E=3.00$ for the PG model. It is equal to the wall on the exit section 0.386, 0.441, 0.464 respectively for $T_0=1000K, 2000K$ and $3000K$ and equal to 0.358 for the PG case. Note that the increase from T_0 to affect the increase in P/P_0 ratio.

Figure 18 shows the variation of ρ/ρ_0 ratio along the wall of the nozzle giving $M_E=3.00$ for the PG model. It is equal to the wall on the exit section to 0.0761, 0.0764, 0.0763 for respectively $T_0=1000K, 2000K$ and $3000K$ and equal to 0.076 for the PG case. Note that the increase in T_0 affects the increase of ρ/ρ_0 ratio.

The error in each section through the wall of the nozzle is shown in figure 19. Note that the error can go to 2.76% 7.00% 8.30% for $T_0=1000\text{K}$, 2000K and 3000K , which is at the exit section. These values are found when $M_E=3.00$ for the *PG* case. Then errors vary with the variation of M_E and T_0 .

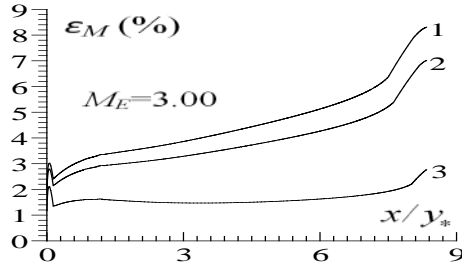


Fig. 19 Variation of the local relative error given by the Mach number on the wall of the *PGMLN*.

Variation on the exit section radius

The figure 20 shows the variation of the Mach number along the radius of the exit section of the nozzle. Variation of the Mach number is determined when $T_0=1000\text{ K}$, 2000 K and 3000 K , respectively shown by the curves 2, 3 and 4. While the curve 1 represents the case for $\gamma=1.402$ for air. Note that it is constant on curve 1 and uniform because the nozzle is determined using the *PG* model so what gives a uniform and parallel flow. For curves 2, 3 et 4, it is noted that the flow is not uniform across the radius of the exit section. A high gradient variation by moving towards the wall of the nozzle is noticed. More T_0 increases, the Mach number on the wall of the nozzle at the exit section decreases.

When $T_0=1000\text{K}$, 2000K and 3000K , the Mach number on the wall at the exit section is respectively equal to 2.918, 2.803 and 2.770. As the Mach number on the axis of symmetry in the exit section is equal respectively to 2957, 2872, 2845. Note that the Mach number at the exit section is no longer constant. So the *HT* model degrades performance including M_E . The *HT* expansion becomes incomplete in the *PG* nozzle. There is a lack of space for complete expansion to $M_E=3.00$. For curves 2, 3 and 4, adjacent to exit section is noted a degradation of Mach number, which justifies the birth of oblique shock wave. This situation is discussed in figure 15.

Figure 21 represents the variation of ratio P/P_0 along the radius of the exit section of the nozzle. For curves 2, 3 and 4, we note that there is increase in this ratio. A high gradient increase by moving towards the wall of the nozzle is noticed. More T_0 increases, the ratio P/P_0 increases gradually.

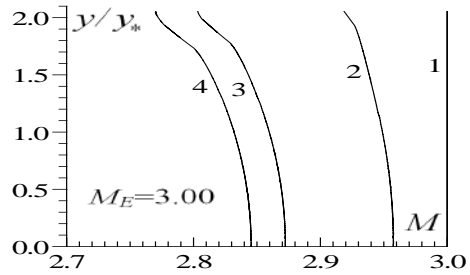


Fig. 20 Variation of the Mach number along the vertical exit section axis of the *PG* axisymmetric *MLN*.

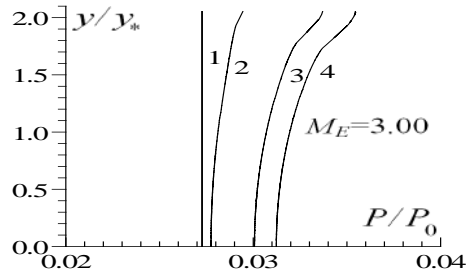


Fig. 21 Variation of the pressure ratio along the vertical exit section axis of the *PG* axisymmetric *MLN*.

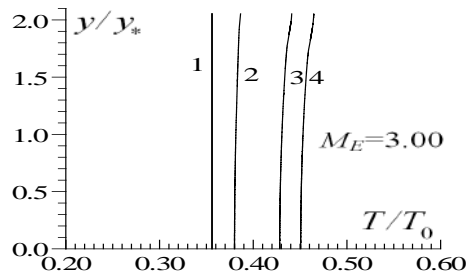


Fig. 22 Variation of the temperature ratio along the vertical exit section axis of the *PG* axisymmetric *MLN*.

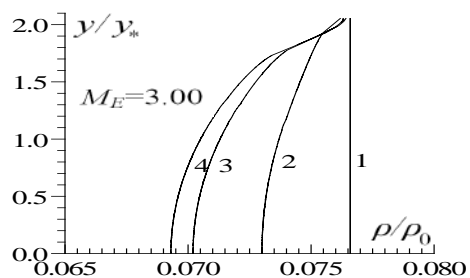


Fig. 23 Variation of the density along the vertical exit section axis of the *PG* axisymmetric *MLN*.

Figure 22 shows the variation of the ratio T/T_0 along the radius of the exit section of the nozzle. For curves 2, 3 and 4, we note that there is increase in this ratio. A high gradient increase by moving towards the wall of the nozzle is noticed.

Figure 23 represents the variation of ratio ρ/ρ_0 along the radius of the exit section of the nozzle. For curves 2, 3 and 4, we note that there is increase in this ratio. A high gradient increase by moving towards the wall of the nozzle is noticed. More T_0 increases, the ratio ρ/ρ_0 increases gradually.

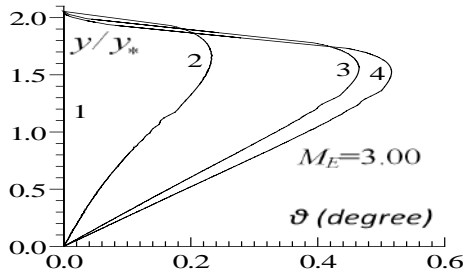


Fig. 24 Variation of θ along the vertical exit section axis of the *PG* axisymmetric *MLN*.

Figure 24 shows the deflection of the flow through the radius of the exit section at *HT*. For the case of an ideal gas, the deviation is represented by line 1 representing $\theta=0.0$ that is to say horizontal flow. While for curves 2, 3 and 4, it is noted that the deflection of the flow is not zero. It is true that at the wall and the axis of symmetry, the deviation is zero whatever the value of T_0 . The maximum deviation is equal to 0.23 degree, 0.46 degree and 0.51 degree, respectively for $T_0=1000\text{K}$, 2000K and 3000K .

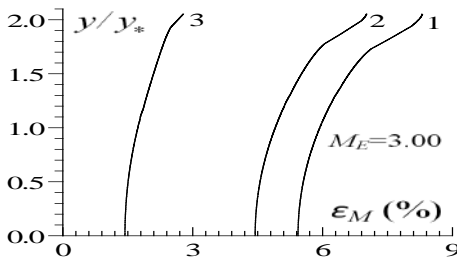


Fig. 25 Variation of ϵ_M given by M on the vertical exit section axis of the axisymmetric *PG MLN*.

The error on Mach number at in each section through the wall of the nozzle is shown in figure 25. Note that the maximum error can go to 2.78%, 7.01% 8.29% for $T_0=1000\text{K}$, 2000K and 3000K which is located at the wall. These values are found when $M_E=3.00$ of *PG* model. Then errors vary with the variation of M_E and T_0 .

Results for *HT* model

The maximum error between all calculation parameters is found for the pressure ratio across the axis of symmetry at the end of the Kernel region. $T_0=3550\text{K}$ and $M_E=5.00$ (extreme *HT* or extreme supersonic), the maximum error of the *PG* model compared to *HT* model can reach $\epsilon_{\text{Computation}}=54,46\%$.

Figure 26 shows the variation of the coefficient C_F at *HT* of the nozzle based on M_E . If the gas is considered as *HT*, the ratio P/P_0 , as shown in figure 26 increases through the wall of the nozzle if T_0 increases. As P/P_0 ratio affects the coefficient C_F , then we will have an increase this coefficient. When $M_E=3.00$, the coefficient C_F takes the values of 0.301, 0.328, 0.335 respectively for $T_0=1000\text{K}$, 2000K and 3000K and 0.298 for the *PG* model.

Figure 27 shows the overall error of the *PG* model from the model *HT* on the C_F coefficient according to M_E . $M_E=3.00$, errors are equal to 3.55%, 8.87% and 10.82% for $T_0=1000\text{K}$, 2000K and 3000K . It is clearly seen that the error increases with increasing of T_0 , and T_0 increases plus *PG* model a way from *HT* model. If we accept an error of 5% between the two models, we can use the *PG* model in stead of *HT*, if $T_0 < 1000\text{K}$ about whatever M_E or $M_E < 1.33$ is some T_0 .

Figure 28 represents the variation at *HT* of the coefficient C_F according to T_0 , when $M_E=3.00$. Note clearly the correction made by the effect of temperature on the *HT* model, as the curve 2 showed it. *PG* model does not depend on T_0 as indicated by the curve 1.

Figure 29 shows the corresponding iso-Mach curves for $M=2.50$ for different values of T_0 in the nozzle giving $M_E=3.00$ for *PG* model. We note that there is deceleration of the flow when they are considered as *HT*. That is to say, the *PG* model tends to further increase the Mach number through the nozzle to the exit section. For this reason the *HT* isochore Mach arrives faster at the exit section relative to the iso-*PG* Mach curve. Therefore by *HT* flow is faster than the flow in *PG*. Then, the flow to the *HT* exit section arrives with a Mach number lower as compared to the *PG* model.

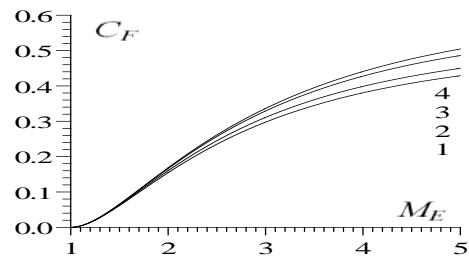


Fig. 26 Variation at *HT* of C_F versus M_E for the axisymmetric *PG MLN* giving M_E at the exit section.

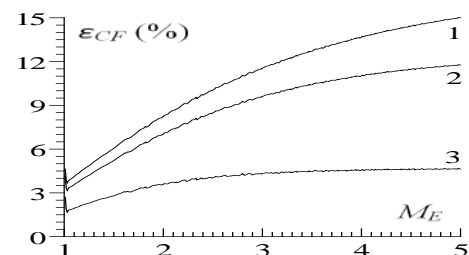
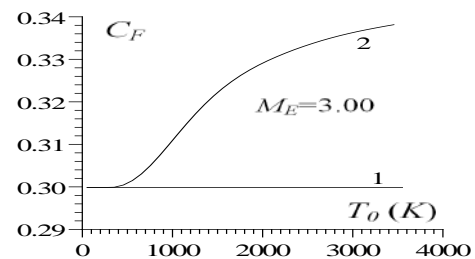


Fig. 27 Variation of the relative error given by C_F of the axisymmetric *PG* model versus M_E .



Curve 1 : *PG* Model ($\gamma=1.402$) ($M_E=3.00$)

Curve 2 : *HT* Model for ($M_E=3.00$)

Fig. 28 Variation at *HT* of C_F versus T_0 of the axisymmetric *PGMLN* giving M_E at the exit section.

Table 1 represents the Mach number that will exist on the exit section when T_0 is taken into account. It is noted that the M_E will remain more uniform because it is not the same on the wall and to the horizontal axis. M_E can still be seen that on the axis of symmetry is greater than that on the wall, which demonstrates the existence of a shock wave and in addition the trajectory of a particle on the axis is shorter than that along the wall. More T_0 increases it more degradation of M_E . Then use the model *HT* disappear the flow uniformity at the exit section. If $T_0 < 1000K$, regardless of M_E , or $M_E < 1.50$ regardless of T_0 , we notice that there is almost no difference between the *HT* and *PG* models, which demonstrate the using of *PG* model for calculation.

Table 1 : Mach number at *HT* on the exit section for *PG* axisymmetric *MLN*.

<i>PG</i>	<i>HT</i>					
	$T_0=1000\text{ K}$		$T_0=2000\text{ K}$		$T_0=3000\text{ K}$	
	Wall	Axis	Wall	Axis	Wall	Axis
1.00	1.000	1.000	1.000	1.000	1.000	1.000
1.50	1.485	1.488	1.477	1.481	1.474	1.480
2.00	1.964	1.974	1.935	1.952	1.926	1.945
2.50	2.440	2.462	2.376	2.414	2.357	2.400
3.00	2.920	2.955	2.804	2.871	2.769	2.844
3.50	3.403	3.451	3.227	3.325	3.173	3.278
4.00	3.887	3.947	3.655	3.785	3.572	3.705
4.50	4.374	4.444	4.093	4.249	3.972	4.131
5.00	4.859	4.939	4.540	4.718	4.377	4.559

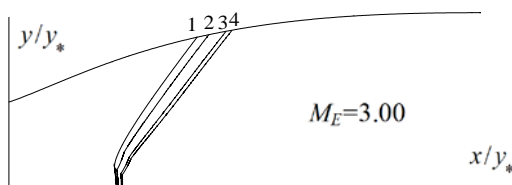


Fig. 29 IsoMach curves of $M=2.50$ in *PGMLN*.

CONCLUSIONS

From this study, we can write the following conclusions. May choose other material instead of air. Relations remain valid. We need to have $C_P(T)$, R of the gas. At low temperature and Mach number, the difference in results between the two models is small, which gives the opportunity to study a *HT* flow using *PG* relationships. Use of *PG* model for the design of supersonic nozzles degrades the performance of the actual design parameters when T_0 is high. The flow to the exit section is neither uniform nor remains parallel. An oblique shock wave is developed on the wall near the exit section of the nozzle *PG* model. This shock wave than to the throat if T_0 increases. The flow field in the nozzle remains no longer divided into three zones

as the case of the *PG* model, it will consist solely of a single flow area not simple type. While no uniform region. The shape of the nozzle of the *PG* model is given as tabulated values. Then an interpolation is necessary to find an analytical form of the nozzle. In our study. We used the cubic spline interpolation. Actually, most T_0 is high; the expansion in the nozzle of the *PG* model will be incomplete. The committed error by the *PG* model over the *HT* model increases more T_0 will be high. A correction to the shape of the nozzle for *PG* model is necessary if we keep the same design parameters and that depending on the value of T_0 . Beyond this limit we will dissociation of molecules. The results are presented for the case of air when $M_E=3.00$ and $T_0=1000K, 2000K$ and $3000K$. This study remains valid in the intervals $55K \leq T_0 \leq 3550K$ and $1.00 < M_E \leq 5.00$. The experimental study of flow in a supersonic nozzle formed by the nozzle of figure 1 will be misrepresented because the upstream conditions for the Mach number will be neither uniform nor parallel, especially if T_0 is high. As a solution, we need to find another form of the geometry of the nozzle which provides a uniform and parallel flow that meets the high values of T_0 .

At the end of this work and to complete the study in this research include some interesting following works.

- Correct the flow in the nozzle *MLN* dimensioned by the *PG* model using there solution of the Euler equations with a new form of energy equation taking into account the variation of the $C_P(T)$.
- We can do the calculation of the flow with other gas instead of air. Here we must determine the function $C_P(T)$ and R of the substance.
- Calculate the intensity of noise generated by the flow in the *MLN* nozzle.

ACKNOWLEDGMENT

The authors acknowledges Khaoula, AbdelGhani Amine, Ritadj and Assil Zebbiche and Mouza Ouahiba for granting time to prepare this manuscript.

REFERENCES

Anderson Jr., J. D., "Fundamentals of Aerodynamics," Mc Graw-Hill Book Company, New York. (1982).
 Anderson Jr. J. D., "Modern Compressible Flow: With Historical Perspective," Mc Graw-Hill Book Company, New York, (1988).
 Argrow B. M. and Emanuel G., "Comparison of Minimum Length Nozzles," Journal of Fluid Engineering, Vol. 110, PP. 283–288, (1988).
 Berger M., "Geometrie: Convexes et Polytopes, Polyèdres réguliers, aires et Volumes," Tome 3, Fernand Nathan, Paris, (1978).
 Demidovitch B. and Maron I., "Eléments de calcul numérique," Edition MIR, Moscou, (1987).

- Dumitrescu L. Z., "Minimum Length Axisymmetric Laval Nozzles," AIAA Journal, Vol. 13, PP. 520–532, (1975).
- Emanuel G., "Gasdynamic: Theory and Application. AIAA Educational Series, New York, (1986).
- Fletcher C. A. J., "Computational Techniques for Fluid Dynamics: Specific Techniques for Different Flow Categories," Vol. II, Springer-Verlag, Berlin, Heidelberg, (1988).
- McLain D. H., "Drawing contours from arbitrary data points," Computer Journal, Vol. 17, PP. 318–324, (1974).
- Oosthuisen P. H. and Carscallen W. F., "Compressible Fluid Flow," Mc Graw-Hill, New York, (1997).
- Peterson C. R. and Hill P. G., "Mechanics and Thermodynamics of Propulsion," Addition-Wesley Publishing Company Inc., (1965).
- Raltson A. and Rabinowitz A., "A First Course in Numerical Analysis," McGraw Hill Book Company, (1985).
- Zebbiche T. and Youbi Z., "Supersonic Plug Nozzle Conception and Comparison to the MLN Configuration," Journal of Aerospace Sciences and Technologies, Vol. 58, N° 3, PP. 184-196, August (2006).
- Zebbiche T., "Stagnation temperature effect on the Prandtl Meyer function," AIAA Journal, Vol. 45, N° 4, PP. 952–954, (2007a).
- Zebbiche T. and Youbi Z., "Effect of stagnation temperature on the supersonic flow parameters with application for air in nozzles," The Aeronautical Journal, Vol. 111, N° 1115, PP. 31–40, (2007b).
- Zebbiche T. and Youbi Z., "Supersonic two-dimensional minimum length nozzle design at high temperature. Application for air," Chinese Journal of Aeronautics, Vol. 20, N° 1, PP. 29–39, (2007c).
- Zebbiche T. and Youbi Z., "Effect of Stagnation Temperature on the Supersonic Two-Dimensional Plug Nozzle Conception. Application for Air," Chinese Journal of Aeronautics, Vol. 20, N° 1, PP. 15-28, February (2007d).
- Zebbiche T., "Stagnation temperature effect on the supersonic axisymmetric minimum length nozzle design with application for air," Advances in Space Research, Vol. 48, PP. 1656–1675, (2011).
- Zebbiche T. and Boun-jad M., "Numerical quadrature for the Prandtl—Meyerfunction at high temperaturewith application for air," Thermophysics and Aeromechanics, Vol. 19, N° 3, PP. 381–384, (2012).
- Zucker R. D. and Bilbarz, O., "Fundamentals of Gasdynamics," John Wiley & Sons, New York, (2002).
- Zucro M. J., Hoffman, J. D., "Gas Dynamics," Vol. 1 and 2, John Wiley, New York, (1976).
- x Abscissa of a point.
- y Radius of a point.
- a Speed of sound.
- P Pressure.
- T Temperature.
- L Length of the nozzle sized on the use of PG model
- S Curvilinear length.
- R Thermodynamic constant of air.
- H Enthalpy.
- C_P Specific heat at constant pressure.
- NC Number of regular characteristics down to the nozzle MLN .
- NJ Descending number of characteristics included in the region of Kernel.
- μ Mach angle.
- θ Deviation of the velocity vector.
- γ Specific heats ratio.
- ρ Density.
- ε Error caused by the PG model over the HT model.
- ξ, η Downward and upward Mach lines.
- C_F Thrust coefficient.

Abbreviations

- HT High Temperature.
- PG Perfect Gas.
- MLN Minimum Length Nozzle.
- MOC Method Of Characteristics.
- C^+ Upward characteristic.
- C^- Downward characteristic.

Subscripts

- 3 Value at point 3.
- 0 Stagnation condition (combustion chamber).
- * Critical condition.
- E Exit section.

NOMENCLATURE

- M Mach number.